Article

New Insight into Modeling Non-Covalently Imprinted Polymers

Hyunjung Kim, and David A. Spivak

J. Am. Chem. Soc., **2003**, 125 (37), 11269-11275• DOI: 10.1021/ja0361502 • Publication Date (Web): 23 August 2003

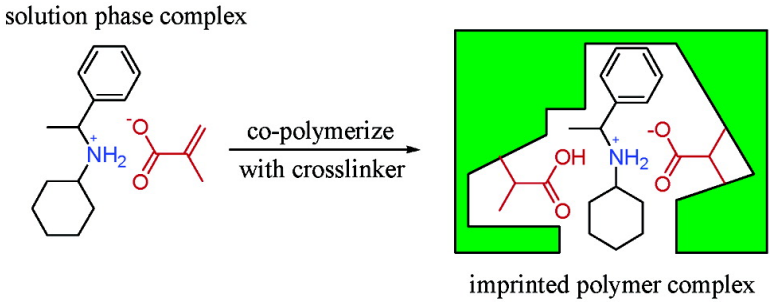

More About This Article

Additional resources and features associated with this article are available within the HTML version:

- Supporting Information
- Links to the 3 articles that cite this article, as of the time of this article download
- Access to high resolution figures
- Links to articles and content related to this article
- Copyright permission to reproduce figures and/or text from this article

View the Full Text HTML

J|A|C|S
ARTICLES
Published on Web 08/23/2003

New Insight into Modeling Non-Covalently Imprinted Polymers

Hyunjung Kim and David A. Spivak*

Contribution from the Department of Chemistry, Louisiana State University, Baton Rouge, Louisiana 70803

Received May 14, 2003; E-mail: David_Spivak@chem.lsu.edu

Abstract: Three series of polymers were carefully formulated with increasing amounts of template while keeping the polymer components constant. The number of binding sites (N) and the number average association constant (K_n) were calculated for each polymer in a series, using equations adapted from the literature describing molecularly imprinted polymers (MIPs). The trends of N and K_n for each series of polymers, which were graphed versus percent template, suggest multiple functional monomers in the binding sites of noncovalent MIPs. This new insight has implications for understanding the underlying mechanisms for the formation of binding sites in the MIPs studied.

Introduction

Molecularly imprinted polymers (MIPs) are actively being developed as a practical tool for affinity chromatographic supports, catalysts, and sensor materials.[1−3] The ease of formation and stability of MIPs may find them to be of more practical use for these and other applications versus synthetic small molecules or biomolecules. The model outlined in Scheme 1 is most widely used to explain the formation of molecularly imprinted binding sites. First, functional monomers are preorganized about a template molecule and "locked" into place by copolymerization with a cross-linking monomer. Removal of the template affords a polymer with specific binding sites for the template. Because the MIP materials are amorphous, crystallographic or microscopy methods cannot be used to determine the structure of the MIP binding sites. Early binding data analyses have indicated that MIPs have a heterogeneous distribution of binding sites comprised of lower affinity to higher affinity sites within the same polymer.[4] Recently, advances in characterization of MIP binding data have afforded a more accurate picture of the binding site distribution and its impact on binding and selectivity values.[5−7] Using new MIP characterization methods, this study probes the effects of changing template concentration on the binding performance of MIPs.

Noncovalent formation of the prepolymer complex (PPC) is most often employed for introducing functionality into MIPs because of easier methodology and greater numbers of high affinity sites, versus covalent methods. The primary consideration associated with the noncovalent approach is maximization

Scheme 1. Outline of the Molecular Imprinting Process

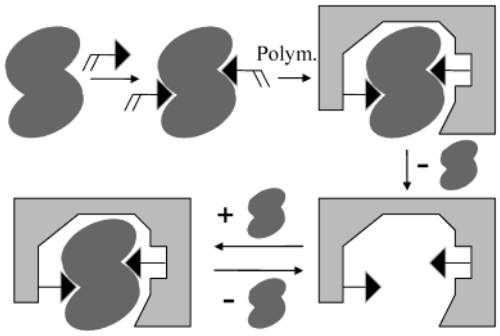

of the PPC, which is in equilibrium with its component parts. One way to increase the PPC concentration is to increase the amount of functional monomer. Another option for increasing the PPC concentration is to increase the amount of template. In fact, the template can in principle be increased indefinitely without affecting the final formulation of the polymer, since the template is all removed at the end of the imprinting process. Thus, the PPC can, in theory, be driven virtually to its full complex state by using the template in large amounts, while maintaining a desired cross-linker to functional monomer (XL/FM) ratio. This strategy has been utilized by Andersson and co-workers, who imprinted the template nicotine at various concentrations while keeping the monomer amounts and the XL/FM ratio constant.[8] The data obtained from the analysis of these polymers showed that maximizing the amount of template did not optimize the MIP performance; instead, the peak performance was found to be closer to a 4:1 monomer:template ratio. From these data, the authors proposed a hypothetical model for one-point binding, two-point binding, and multipoint binding to account for the data observed. We have performed a similar investigation using simpler templates for which only one solution complex is expected and compared the results to an

(1) Wulff, G. *Angew. Chem., Int. Ed. Engl.* **1995**, *34*, 1812−1832.
(2) Shea, K. J. *Trends Polym. Sci.* **1994**, *2*, 166−173.
(3) Ekberg, B.; Mosbach, K. *Trends Biotechnol.* **1995**, *13*, 47−51.
(4) Wulff, G.; Grobe-Einsler, R.; Vesper, W.; Sarhan, A. *Makromol. Chem.* **1977**, *178*, 2817−2825.
(5) Umpleby, R. J., II; Baxter, S. C.; Bode, M.; Berch, J. K., Jr.; Shah, R. N.; Shimizu, K. D. *Anal. Chim. Acta* **2001**, *435*, 35−42.
(6) Umpleby, R. J., II; Bode, M.; Shimizu, K. D. *Analyst* **2000**, *125*, 1261−1265.
(7) Szabelski, P.; Kaczmarski, K.; Cavazzini, A.; Chen, Y. B.; Sellergren, B.; Guichon, G. *J. Chromatogr., A* **2002**, *964*, 99−111.
(8) Andersson, H. S.; Karlsson, J. G.; Piletsky, S. A.; Koch-Schmidt, A.-C.; Mosbach, K.; Nicholls, I. A. *J. Chromatogr., A* **1999**, *848*, 39−49.

equivalent nicotine imprinted polymer series. Batch rebinding studies were performed in order to obtain equilibrium binding values which were evaluated using the Freundlich binding model, from which the distribution of binding affinities and number of binding sites were obtained. The outcome of this study suggests a more complete model for explaining how binding sites are formed by the molecular imprinting method.

Computational Methods

Through a series of elegant papers by the groups of Shimizu,[5] Sellergren, and Guichon,[7] the Freundlich equation has been determined to be a suitable binding isotherm model for MIPs, which is used in this study. Once the appropriate Freundlich equation is found with an acceptable fit to the binding isotherm data, the equation for the affinity distribution can be written incorporating the parameters of the Freundlich equation, A and ν:[7]

$$N(K_i) = A\frac{\sin(\pi\nu)}{\pi}K_i^{-\nu} \quad (1)$$

Furthermore, assuming that the number of binding sites is high enough to take the limit $N \rightarrow \infty$ (thermodynamic limit), the value of the association constant of a given site is equal to the reciprocal of the free concentration of the substrate (C_f):

$$K_i = 1/C_f \quad (2)$$

This allows determination of the K_i values experimentally for eq 1, to give eq 3.

$$N(K_i) = A\frac{\sin(\pi\nu)}{\pi}K_i^{-\nu}|_{K_i = 1/C_f} \quad (3)$$

The graph of eq 3 (in terms of N vs ln K) represents the affinity distribution, and the area under this curve gives the total number of binding sites. By integrating eq 3, we obtain a new function which calculates the area under the curve and thus N, the total number of binding sites (eq 4).

$$N = \int_{\ln K_{min}}^{\ln K_{max}} N(K_i)\, d(\ln K) = \frac{A\sin(\pi\nu)}{\pi}(K_{min}^{-\nu} - K_{max}^{-\nu}) \quad (4)$$

However, it should be noted that this area is the number of binding sites for the specified range of affinity constant values, that is, the range between K_{min} and K_{max}.

To obtain the number average association constant (for a specified range of $K_{min} - K_{max}$), a relationship is developed in a fashion similar to that for determining the number average molecular weight (M_n) of a polymer. For the number average molecular weight of polymers, the sum of all sites N_i multiplied by the corresponding affinity constant, K_i, is divided by the sum of N_i, which is the total number of sites N (eq 5).

$$\Sigma N_i K_i / \Sigma N_i = \Sigma N_i K_i / N \quad (5)$$

From the continuous affinity distribution of the graph of eq 3 (in terms of N vs ln K), $\Sigma N_i K_i$ can be substituted by the integration of the product of the number of binding sites for each class with its corresponding association constant, shown as the numerator of eq 6. When this is divided by the number of binding sites N from eq 4, the number average association constant (K_n) is obtained.

$$K_n = \frac{\int_{\ln K_{min}}^{\ln K_{max}} N(K_i)K_i\, d(\ln K)}{\int_{\ln K_{min}}^{\ln K_{max}} N(K_i)\, d(\ln K)} \quad (6)$$

After substitution of eq 3 in the numerator and denominator, followed by integration, we obtain the following solution for the number average association constant:

$$K_n = \frac{\nu}{1-\nu}\frac{(K_{max}^{1-\nu} - K_{min}^{1-\nu})}{(K_{min}^{-\nu} - K_{max}^{-\nu})} \quad (7)$$

From eq 7, the number average association constant can be calculated using a binding isotherm that is modeled by the Freundlich equation.

Results and Discussion

The objectives of this study required a series of polymers to be imprinted with increasing amounts of template, keeping the monomer (and initiator) concentration constant. This has been previously carried out using the template nicotine, and we recreated that system for this study.[8] Nicotine has two amine functional groups, which are capable of multiple interactions that must be accounted for when modeling the system, complicating the overall understanding of the model. We were also interested in studying a system with one amine which was anticipated to provide an easier model to understand. For this purpose, cyclohexyl(phenylethyl)amine (CPA) was chosen as a template with a single amine group and a chiral center much like nicotine and is a liquid for solvating monomers and initiator in MIP formulations. To verify a generality of results for templates incorporating a single amine, a second series of polymers were imprinted using cyclohexyl(naphthylethyl)amine (CNA).

Stoichiometry of Solution Phase Prepolymer Complexes. The assembly of functional groups around the template in the solution, that is, formation of prepolymer complex, is the first step in the imprinting scheme (Scheme 1). The presence and stoichiometry of prepolymer complexes were determined by Job's plots of MAA with all three templates, (*S*)-CPA, (*S*)-CNA, and (*S*)-nicotine (Figure 1).[9] Solutions of template and functional monomer were formulated such that the combined concentration of MAA and template substrates (C_0) were kept at constant molarity, but the relative molar fractions of MAA and the template substrates were varied in a compensatory manner to establish the Job's plot. The complex concentration was calculated using the product $(\delta_{obs} - \delta_T)f_T$,[10] where $(\delta_{obs} - \delta_T)$ is the change in chemical shift of the methyl protons of the pyrrolidine ring ((*S*)-nicotine) or the amine protons of the template ((*S*)-CPA or (*S*)-CNA) in the presence of MAA and f_T is the molar fraction of the template. Different values of C_0 were used to plot the complex concentration versus the molar fractions of MAA at concentrations above the necessary threshold value.[10] The Job plot for (*S*)-CPA (Figure 1a) shows that a maximal complex was formed at a 0.5 molar fraction of MAA for all values of C_0. This result provides evidence for the formation of a 1:1 complex between functional monomer MAA and the template (*S*)-CPA in solution. (*S*)-CAN substrates also formed a 1:1 complex with MAA as shown in Figure 1b. On the other hand, for (*S*)-nicotine substrates, the Job plot shows a maximal complex at a 0.6 molar fraction of MAA confirming the formation of a 1:2 complex between (*S*)-nicotine substrates and MAA (Figure 1c).

(9) Huang, C. Y. *Methods Enzymol.* **1982**, *87*, 509−525.
(10) Schneider, H.; Yatsimirsky, A. *Principles and Methods of Supramolecular Chemistry*; John Wiley & Sons: West Sussex, U.K., 2000.

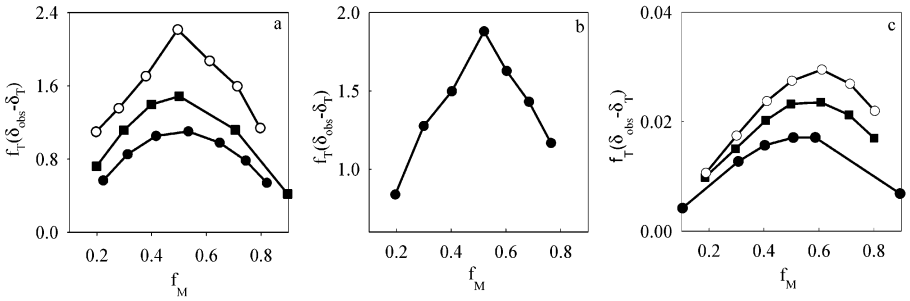

Figure 1. Job's plots for the association between MAA and (a) (*S*)-CPA substrates in $CDCl_3$ at the combined concentration of MAA and (*S*)-CPA substrates of 20mM(●), 40mM(■), and 60mM(○); (b) (*S*)-CNA substrates in $CDCl_3$ at the combined concentration of MAA and (*S*)-CNA substrates of 30mM; and (c) (*S*)-nicotine substrates in $CDCl_3$ at the combined concentration of MAA and (*S*)-CNA substrates of 40mM(●), 80mM(■), and 160mM(○).

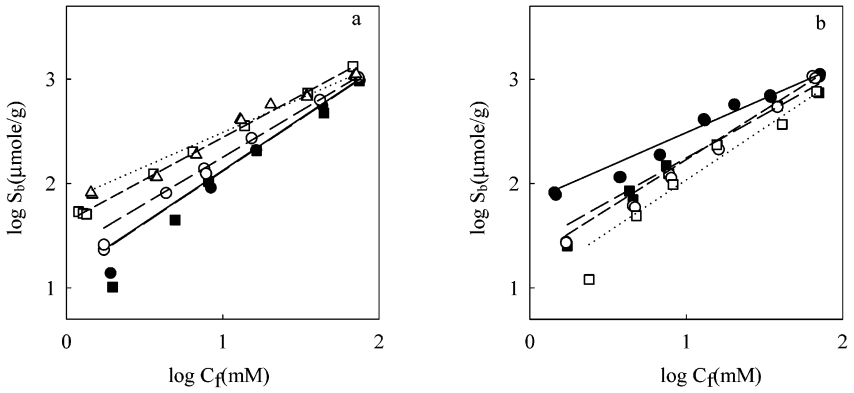

Figure 2. Binding isotherms for (a) Region I, (*S*)-CPA MIPs with 0% (−●−), 1% (--■--), 2% (--○--), 5% (--□--), and 10% (···△···) and binding isotherms for (b) region II (*S*)-CPA MIPs with 10% (−●−), 20% (--■--), 50% (--○--), and 100% (···□···) in log−log format. The symbols represent experimental data, while the solid lines are their fits calculated by the Freundlich equation. The rebinding medium was MeCN/HoAc (95:5, v/v). The amount of the polymer was 0.1 g. UV detected the free concentration of the substrates for (*S*)-CPA at 260 nm.

Table 1. Polymer Compositions

polymer entry	(1)	(2)	(3)	(4)	(5)	(6)	(7)	(8)
mole % template	0	1	2	5	10	20	50	100
mmol template	0	0.32	0.64	1.58	3.16	6.31	15.78	31.55
mmol MAA	6.31	6.31	6.31	6.31	6.31	6.31	6.31	6.31
mmol EGDM	25.2	25.2	25.2	25.2	25.2	25.2	25.2	25.2
vol of $CHCL_3$, mL [for (*S*)-nicotine and (*S*)-CPA]	8	7.93	7.86	7.65	7.30	6.59	4.48	0.97
vol of $CHCL_3$, mL [for (*S*)-CNA]	12	11.92	11.85	11.62	11.25	10.49	8.23	4.45
mmol AIBN	0.64	0.64	0.64	0.64	0.64	0.64	0.64	0.64

Polymer Imprinting and Binding Studies. A series of polymers for each template was synthesized using increasing amounts of template with the conditions for each polymer listed in Table 1. The extra volume provided by the template in each case was compensated for by a reduction in solvent volume to maintain the same overall polymerization volume. Polymers were extracted with methanol and sized to the range 25−38 μm, and the binding was evaluated by batch rebinding studies.

For the batch rebinding experiments, a constant volume of a solution with various concentrations of template was added to a fixed amount of the polymer and shaken for 24 h allowing equilibrium to be reached. The amount of free template (C_f, mM) was determined by measuring the UV absorbance of the supernatant, and the amount of bound template (C_b, mM) was determined by subtracting the amount of free template from the total amount of template (i.e., $C_b = C_T - C_f$) added to the polymer solution. A plot of C_b versus C_f is often used to graph the binding isotherms for imprinted polymers. Because the polymers are solid, C_b is converted to S_b which has dimensions in micromoles of substrate per gram of polymer (μmol/g). Therefore, the binding isotherms for the polymers are plotted as S_b versus C_f. As previously mentioned, it has been shown that MIP isotherms fit well to the Freundlich equation.[5] The Freundlich equation is an exponential model that is best represented in a log S_b versus log C_f format, which is used to graph the isotherms presented in Figure 2. For each of the three templates, eight isotherms are obtained for each of the MIP formulations employing increasing amounts of template. The isotherms for the polymers imprinted with (*S*)-CPA are shown in Figure 2; isotherms for the MIPs to the other templates can be found in the Supporting Information. The eight isotherms are divided into two different graphs; region I for those with 0%, 1%, 2%, 5%, and 10% template [Figure 2a for (*S*)-CPA] and region II for those with 10%, 20%, 50%, and 100% template [e.g., Figure 2b for (*S*)-CPA]. Region I illustrates the upward movement (indicating increasing binding ability) of the isotherms from 0−10% template, whereas region II illustrates a downward movement (indicating decreasing binding ability) from 10−100% template. In addition to trends in binding ability, Figure 2 also illustrates good linearity, supporting the Freundlich model of binding isotherm. Thus, from this point on, the Freundlich equation found for each isotherm will be used to calculate the affinity distribution and total number of binding sites.

Affinity Distributions. The experimental binding isotherm (S_b vs C_f) was first fitted with a Freundlich isotherm:[5] $S_b = AC_f^{\nu}$. Then, using the software program SigmaPlot 7.101,[11] the

(11) SPSS Inc. Headquarters, 233 S. Wacker Drive, 11th floor Chicago, IL 60606.

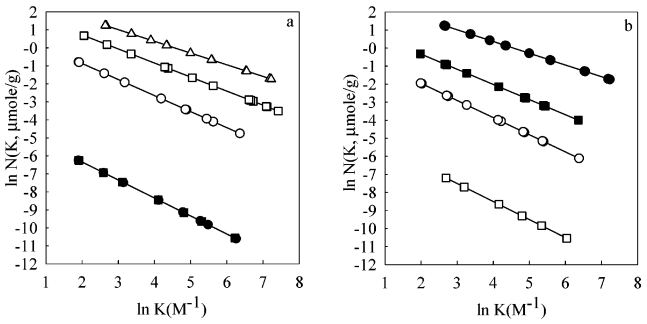

Figure 3. Affinity distributions for (a) region I, (*S*)-CPA MIPs with 0% (●), 1% (■), 2% (○), 5% (□), and 10% (△) and affinity distributions for (b) region II (*S*)-CPA MIPs with 10% (●), 20% (■), 50% (○), and 100% (□) in log−log format. Values for *K* were approximated by choosing experimental determined values of free concentration of S-substrate ($C_f = 1/K$). Values for *N* were then calculated for each value of *K* using eq 3.

best-fit values for *A* and ν were obtained by varying these parameters one at a time and finding the best fit by minimizing the sum-of-squares (SS). The goodness of fit was validated by obtaining correlation constant values (R^2) in the range of 0.972 to 0.999. The standard deviation calculated using SigmaPlot 7.101 was reported as the error in the fitting parameters (*A* and ν).

The fitting parameters *A* and ν were then substituted into the affinity distribution equation (eq 3) and plotted in a ln $N(K_i)$ versus ln *K* format. The affinity distributions for each of the eight different MIPs made with increasing percent of (*S*)-CPA as template are shown in Figure 3; affinity distributions for the other templates can be found in the Supporting Information. The eight affinity distributions are again divided into two different graphs: region I for those with 0−10% template [Figure 3a for (*S*)-CPA] and region II for those with 10−100% template [Figure 3b for (*S*)-CPA]. The behavior of the graphs in Figure 3 are related to the Freundlich fitting parameters *A* and ν. The Freundlich parameter *A* is reflected in an upward movement of the affinity distribution, which represents an apparent increase in the number of binding sites for a specific range of ln *K* values. However, this is not for the entire range of ln *K* values, only for a specified range. Region I in Figure 3 shows an increase in *A* values as the amount of template increases to a maximum at 10%. After the maximum at 10% template, region II shows the *A* values decrease with increasing template.

The Freundlich parameter ν is reflected in the affinity distribution as a change in slope. The parameter ν ranges between 0 and 1, and is used to characterize heterogeneity of binding sites within MIPs.[7] As the values of ν approach 0, the affinity distribution describes more heterogeneous binding sites in the MIPs, and the slope becomes more horizontal. Region I shows a slight change in slope and, thus, ν as the template increases from 0−10%. However, further increasing percent template in region II decreased the heterogeneity of the MIP binding sites.

Number of Binding Sites. The affinity distributions were used to calculate number of binding sites (*N*) using eq 4, using the same K_{min} and K_{max} for each series of MIPs. The number of binding sites found for each MIP in a series was graphed in Figure 4 a−c versus the percent template for (a) (*S*)-CPA, (b) (*S*)-CNA, and (c) (*S*)-nicotine, respectively. The graph can be divided into two regions, region I and region II, which correspond to the regions I and II for the binding isotherms and affinity distributions. Looking at Figure 4a, we find region I shows a continuous increase in the number of binding sites as the template increases from 1% to 10%. The increase in the number of specific binding sites is due to the equilibrium of template and functional monomer complex being driven toward complex formation, which is postulated to be directly responsible for the number of sites formed in MIPs.[12] Region II shows the number of binding sites falls steeply upon going to 20% template and then appears to level off, as at a very low value of specific binding sites, as percent template increases. The data for the (*S*)-CNA MIP series shown in Figure 4b give virtually the same pattern. Region I shows increasing numbers of binding sites until 10% template; however, there is a more gradual decrease in *N* as the percent template increases from 20% to 100%.

The data for the (*S*)-nicotine MIP series is shown in Figure 4c and also furnishes a graph similar to those in Figure 4a and b. This result parallels performance factors, such as selectivity, found for a similar series of (*S*)-nicotine MIPs investigated by Andersson, et al.[8] From their data, Andersson and co-workers suggested an MIP binding site model the correlating number of functional monomers in a binding site versus binding performance. The model is represented as part of Scheme 2, where complex II was hypothesized to exist at low levels of template (relative to functional monomer) and responsible for the most selective binding sites having a functional monomer: template ratio of 2:1. Higher levels of template were postulated to give rise to a class of complexes III, which has an incomplete preorganizaton of functional groups (functional monomer: template ratio of 1:1) which would be responsible for decreased selectivity. Further increase in the level of template would give rise to more and more binding sites with a functional monomer: template ratio of 1:1, explaining the continual decrease in binding performance.

The data from our experiments, shown in Figure 4c, also support a binding site model similar to Scheme 2. The scheme builds on the ideas of Andersson and co-workers, where the increasing template increases the number of binding sites and, thus, increases the performance in MIPs.[8] However, at some maximum value, the number of binding sites appears to decrease. In the case of nicotine, this may be interpreted as a loss of high performance sites which are replaced with inferior sites, resulting in an overall loss of binding capacity. This may also be the case for (*S*)-CPA and (*S*)-CNA discussed next.

The series of MIPs imprinting (*S*)-CPA was anticipated to provide a simpler model of the binding sites versus the nicotine example, since there is only one amine group for interaction with functional monomers. This model was carefully chosen because there are essentially two states, the 1:1 functional monomer:template complex and the uncomplexed template for concentrations of template above 0.003 M in chloroform.[13−16] Therefore, this system should be described by Figure 5, where increasing the amount of template should increase the number of binding sites up to a critical percent template (e.g., 20% template in Figure 5), after which any excess amount of template would be anticipated to have no effect on binding site formation.

(12) Spivak, D. A.; Shea, K. J. *Anal. Chim. Acta* **2001**, *435*, 65−74.
(13) Yeger, E. A.; Barrow, G. M. *J. Am. Chem. Soc.* **1955**, *77*, 4474−4481.
(14) Barrow, G. M.; Yeger, E. N. *J. Am. Chem. Soc.* **1954**, *76*, 5211−5216.
(15) Detar, D. F.; Novak, R. W. *J. Am. Chem. Soc.* **1970**, *92*, 1361−1365.
(16) Barrow, G. M.; Yeger, E. N. *J. Am. Chem. Soc.* **1955**, *77*, 6206−6207.

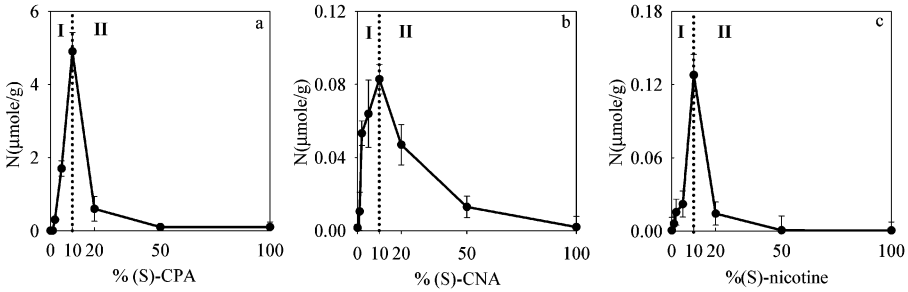

Figure 4. Number of binding sites values (*N*) versus varied percent template for (*S*)-CPA (a), (*S*)-CNA (b), and (*S*)-nicotine (c) MIPs. Values for *N* were calculated using eq 4, and the ranges of association constants used to calculate the values for *N* were 20−500 M^{-1}, 300−10,000 M^{-1}, and 100−10,000 M^{-1} for (*S*)-CPA, (*S*)-CNA, and (*S*)-nicotine MIPs, respectively.

Scheme 2. Postulated Model Relating Complex Structure with Binding Site Structure and the Resulting Quality of Binding Site for Nicotine Imprinted Polymers as Template Concentration is Increased (Adapted in Part from Ref 8)

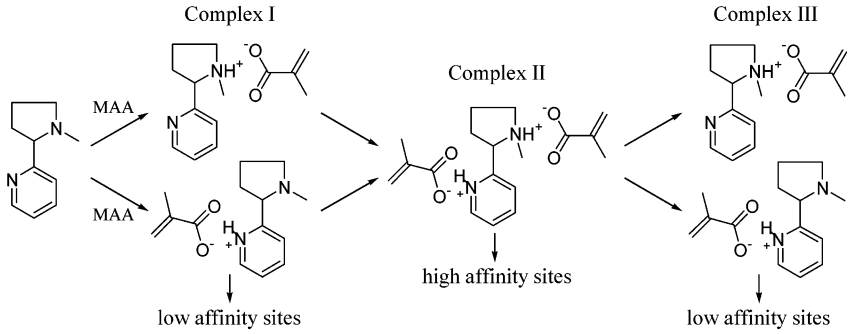

In other words, once all of the functional monomer is complexed, any further addition of template will not have any functional monomer to complex with and, thus, is not expected to increase the number of binding sites. There is also no reason to expect any decrease in the number of binding sites with addition of template, because the equilibrium is driven toward complete complex formation by Le Chatlier's principle. Thus the number of total binding sites would be anticipated to stay the same after this critical amount of template until the maximum 100% template is reached. However, Figure 4a does not have the graph predicted as that in Figure 5, and this same predicament exists for (*S*)-CNA (and Figure 4b versus Figure 5) as well. This dilemma is due to only looking at the number of sites calculated within the limited range of association constants and is resolved by also looking at number average association constants, which is discussed next.

Number Average Association Constant. The number average association constant was calculated according to eq 7 in the Computational Methods section. For each MIP in a series, K_n was graphed in Figure 6a−c versus the percent template of (a) (*S*)-CPA, (b) (*S*)-CNA, and (c) (*S*)-nicotine, respectively. Again, the graphs can be divided into two regions, region I and region II, which correspond to the regions I and II for the binding isotherms and affinity distributions. Region I shows an increase in K_n as the template increases from 1% to 10%, due to the increase in the number of specific binding sites in combination with the simultaneous decrease in the number of nonspecific binding sites that arise from nontemplated functional group orientations. Region II shows a decrease in K_n as the percent template is increased to 20%, which can be explained for nicotine by the model shown in Scheme 2. However, Scheme 2 cannot explain the similar behavior of (*S*)-CPA and (*S*)-CNA in figure 6a and b, because only 1:1 complexes are present in solution. To solve this dilemma, we propose a model for (*S*)-CPA and (*S*)-CNA that is similar to that postulated for nicotine where binding sites with multiple functional monomers can provide higher affinities (Scheme 3). This would suggest that the number of functional monomers in the polymer binding site is determined during the polymerization and *not* as a direct result from the solution phase complex. Thus less specific binding sites would be created as the percent template is increased, resulting in the trends seen in figure 6a and b.

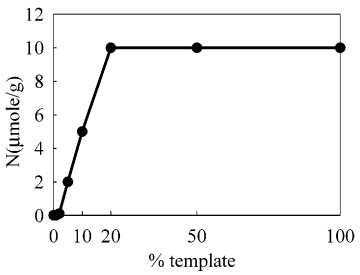

Figure 5. Theoretical behavior predicted for the graph of *N* versus percent template as the template is increased for a model that has only one interaction between the functional monomer and template.

Absence of Morphological Effects. The polymers were characterized to determine if there were any differences between their chemical composition and morphology. One concern with increasing the amount of template was the possibility for leaching of methacrylic acid by the template. This would be more severe as the amount of template increased. Thus, the incorporation of MAA in polymers with different template concentrations was estimated from an abridged survey of four polymers that spanned the full range of template concentrations. The FTIR spectra in Figure 7 for each of the polymers in the survey show the characteristic peak for MAA in the range of 3300−3500 cm^{-1} which corresponds to the carboxylate OH stretch. Using the ratio of the area under the carboxylate OH peak in the IR over that found for the C−H peak from the glycol

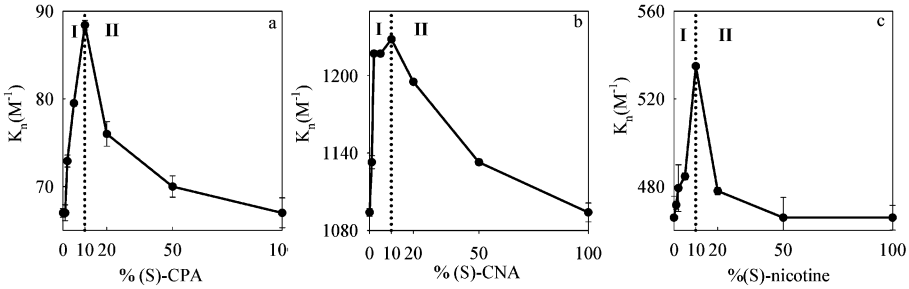

Figure 6. Number average association constant values (K_n) for (a) (*S*)-CPA, (b) (*S*)-CNA, and (c) (*S*)-nicotine MIPs. Values for K_n were calculated using eq 7, and the ranges of association constants used to calculate the values for K_n were 20−500 M^{-1}, 300−10 000 M^{-1}, and 100−10 000 M^{-1} for (*S*)-CPA, (*S*)-CNA, and (*S*)-nicotine MIPs, respectively.

Scheme 3. New Model Proposed to Relate Complex Structure with Binding Site Structure and the Resulting Quality of Binding Site for Singly Functionalized Templates Such as (*S*)-CPA, Based on the Data in Figures 4 and 6

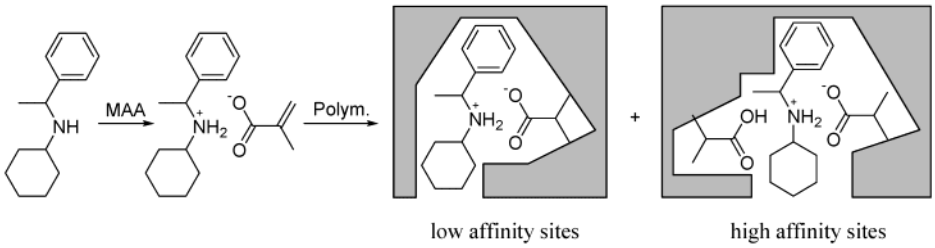

unit of EGDMA at 950 cm^{-1} (which was used as an internal standard), the MAA content of the different polymers was compared (Table 2). The data in the second column of Table 2 show the relative amounts of MAA to EGDMA give roughly the same values; the higher the ratio, the greater the content of MAA versus EGDMA. Thus it can be concluded that the chemical compositions of the different MIPs are roughly the same, with no leaching of functional monomer as the percent template is increased. Furthermore, the degree of cross-linking determined from the ratio of the vinyl C−H peak over the internal standard (third column in Table 2) shows that all MIPs have roughly the same degree of pendant double bonds from un-cross-linked EGDMA. Thus, even though increasing the amount of template changes the distribution of monomers in the MIPs, the polymer composition and degree of cross-linking are unaffected.

Table 2. FTIR Analysis of Different (*S*)-CNA Imprinted Polymers

% template	normalized –OH peak area from the carboxylic acid[a]	normalized vinyl C–H peak area[b]
0	8 ± 1.1	0.64 ± 0.077
1	10 ± 2.3	0.7 ± 0.12
10	11 ± 1.0	0.57 ± 0.019
100	15 ± 1.7	0.72 ± 0.057

[a] The net peak area of the carboxylic acid OH stretch was determined in the absorbance mode between the integration limits of 3750 and 3250 cm^{-1}, and this net area was normalized against a net reference with integration limits between 990 and 920 cm^{-1}. [b] The net peak area of a vinyl proton was determined in the absorbance mode between the integration limits of 1660 and 1580 cm^{-1}, and this net area was normalized against a net reference with integration limits between 990 and 920 cm^{-1}.

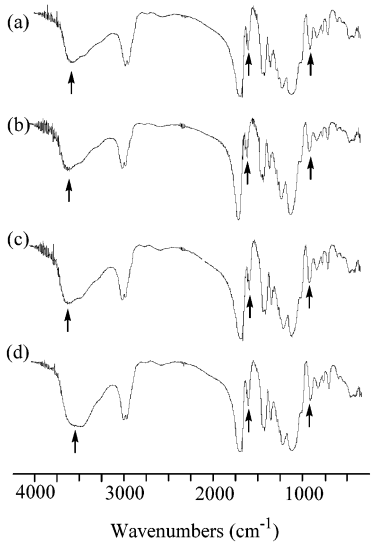

Figure 7. FTIR spectra of polymers with (a) 0%, (b) 1%, (c) 10%, and (d) 100% template. The arrow at 950 cm^{-1} indicates the C−H stretch of the glycol unit of EGDMA, and the arrow at the broad band around 3440 cm^{-1} indicates the O−H stretch of the carboxylate group of MAA. The arrow at 1639 cm^{-1} indicates the vinyl C−H bending, which is a measure of the unreacted double bonds of EGDMA.

Changing the amount of template in each series not only affects the distribution of aggregate complexes but also plays a role in determining the final pore structure of the polymers. The surface area and porosity in the MIP network polymers are influenced by the presence of solvent (referred to as "porogen") during polymerization.[17] The porogen undergoes phase separation during polymerization and creates "pools" or "tunnels" that eventually become the pore architecture within the network polymer matrix. A poor solvent (i.e., theta solvent) phase separates early in the polymerization leaving larger pores and modest-to-large surface areas. On the other hand, good solvents such as chloroform used in this study do not phase separate well and limit the porosity providing low surface areas. Figure 8 shows the change in surface area vetsus the percent template of (*S*)-CPA with increasing amounts of template. From 0−20%, chloroform is the dominant porogen, which is reflected in the low porosity and surface area seen in this range. (*S*)-CPA, and any other polar solvent, is a poor solvent and would

(17) Guyot, A. *Synthesis and Separations using Functional Polymers*; Sherrington, D. C., Hodge, P., Ed.; John Wiley & Sons: New York, 1989; Chapter 1.

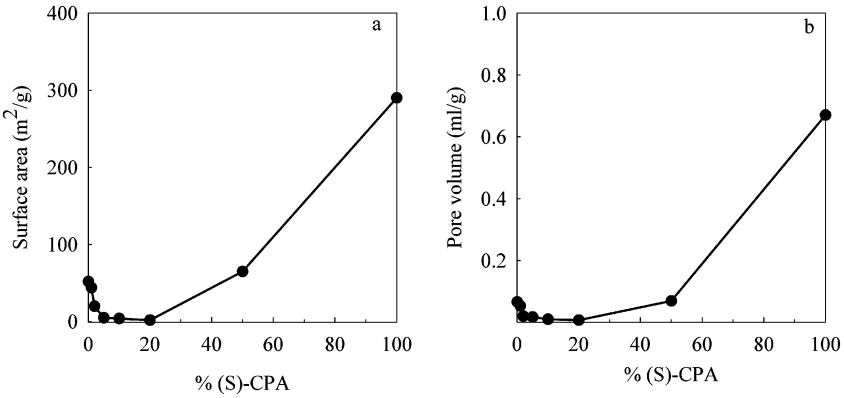

Figure 8. Graphs of (a) surface area (m^2/g) and (b) pore volume (mL/g) versus percent template for (*S*)-CPA MIPs (similar data for the MIPs to (*S*)-CNA and (*S*)-nicotine can be found in the Supporting Information).

be expected to give greater surface area and porosity, as seen in Figure 8 for 20−100% template. In comparing the trends for the number of binding sites (N) and the number average association constant (K_n) with Figure 8a and b, there does not appear to be any correlation of binding properties with surface area or total pore volume. This agrees with earlier porosity studies on MIPs,[18] where there was found to be no correlation of surface area or porosity with MIP performance. Thus, the morphology change in the series of polymers behaves in an understandable fashion and is not expected to influence the binding site structure.

Conclusion

The behavior of noncovalently imprinted polymers was evaluated using the Freundlich model and affinity distribution for a series of polymers with increasing template concentrations. The trends in association constants and numbers of binding sites for each series of polymers are explained by a model that incorporates multiple functional monomers within the binding sites. For polymers imprinted with nicotine, this model has already been proposed based on multiple functional monomers interacting with a single template molecule in the solution phase. On the other hand, for the secondary amine templates in this study, the solution phase complex structure with carboxylate groups has been determined to have a 1:1 stoichiometry of functional monomer:template. A discovery of the studies presented here is that the binding behavior of the polymer binding sites based on the Freudlich equation and affinity distribution is not explained by the 1:1 stoichiometry of the functional monomer:template in solution. This would suggest, at least in the case of (*S*)-CPA and (*S*)-CNA, the number of functional groups in the polymer binding site is not determined directly by the solution phase prepolymer complex; rather, it is determined *during* polymerization. Because of the difficulty in characterizing the binding site structures during and after polymerization, the actual events determining the final binding site structure are still unknown. However, it is reasonable to hypothesize that phase separation phenomena that take place during polymerization could allow for the aggregation of polar functional groups in binding site "pockets", resulting in binding sites with multiple functionalities. The increased number of binding interactions in the polymer binding site may account for a greater fidelity of the site and, thus, impart a greater affinity and selectivity to the site. Thus, the models presented here provide new insight into the underlying mechanisms of MIP binding site formation which could facilitate improvements in MIP process design in the future.

Acknowledgment. This research was supported in part by Research Corporation, through Cottrell Scholar Award CS0801, and an NSF CAREER Program award CHE-0134290 (D.A.S.). We would like to thank Dr. K. D. Shimizu and Dr. R. Umpleby for their assistance with our computational theory. We would also like to thank Benjamin Caire for his assistance with polymer preparation.

Supporting Information Available: Binding isotherms, affinity distributions, pore analysis data for (*S*)-CNA and (*S*)-nicotine polymers, and full experimental details and characterization of molecular compounds and polymers can be found in the Supporting Information. This material is available free of charge via the Internet at http://pubs.acs.org.

JA0361502

(18) Sellergren, B.; Shea, K. J. *J. Chromatogr.* **1993**, *635*, 31−49.